Materials Letters 68 (2012) 350–353

Contents lists available at SciVerse ScienceDirect

Materials Letters

journal homepage: www.elsevier.com/locate/matlet

Synthesis of silver nanoparticles within the pores of functionalized-free silica beads: The effect of pore size and porous structure

Dang Viet Quang [a,c], Pradip B. Sarawade [a], Askwar Hilonga [a], Jong-Kil Kim [b], Young Ho Shim [a], Godlisten N. Shao [a], Hee Taik Kim [a,*]

[a] Department of Fine Chemical Engineering, Hanyang University, 1271 Sa3-dong, Sangnok-gu, Ansan-si, Gyeonggi-do 426-791, Republic of Korea
[b] E&B Nanotech. Co., Ltd., Republic of Korea
[c] Institute of Environmental Technology, Vietnam Academy of Science and Technology, 18 Hoang Quoc Viet, Cau Giay, Hanoi, Viet Nam

ARTICLE INFO

Article history:
Received 14 August 2011
Accepted 20 October 2011
Available online 29 October 2011

Keywords:
Silica beads
Silver nanoparticles
Mesoporous silica

ABSTRACT

Here, we report on the synthesis of silver nanoparticles (Ag-NPs) manipulating the pores of silica beads (SBs) with sizes ranging from 0.5 to 1 mm. Silver ions were occluded inside the pores of SBs and in situ reduced to Ag-NPs using Sodium borohydride ($NaBH_4$). SBs with different average pore diameters from 3.8 to 20 nm were used to assess the effect of their pore sizes and porous structures on the formation of Ag-NPs. Obtained results revealed that the silver amount occluded inside pores increases along with the increase of total pore volume. The particle sizes of the synthesized Ag-NPs mainly distribute from 8 to 15 nm and vary with the pore sizes and porous structure.

1. Introduction

Silver nanoparticles (Ag-NPs) present distinct properties due to their high surface-to-volume ratios, which are not observed in their bulk [1]. Therefore, they have been studied and applied in various fields [2,3], but their applications are usually limited by high cost and workability of nanosized particles. To overcome these drawbacks, silver nanoparticles have been incorporated into various substrates like polymers and inorganic oxide powders [4,5]. Among various substrates, porous silica has proven to be effective to support Ag-NPs [5–9].

Generally, there are two methods to incorporate Ag-NPs into silica substrate, including: (1) impregnation of silver ions into functionalized silica, followed by a reduction process [5–7]; (2) silver ions occluded into functionalized-free silica and then reduced to Ag-NPs [8–10]. In the former method, silica is usually functionalized with a functional group like thiol or amine. This method shows high effectiveness and produces quite homogeneous Ag-NPs [11]; however it requires cost and time for silica surface modification. The latter is relatively popular to synthesize Ag-NPs and nanowires inside pores of mesoporous silica such as MCM-41 and SBA-15, which contain small ordered pores and are favorable to control nanoparticles, but synthesizing technique is complicated and not suitable for applications at large [12–14].

Recently, sodium silicate based silica without surface modification has been studied to support Ag-NPs. Silver ions can be co-precipitated with silica [15] or impregnated into pre-prepared silica [16,17] and then reduced to silver metal. This is a cost effective and facile route to prepare silver nanoparticle. Although several studies have synthesized Ag-NPs and nanowires inside pores of that silica, there is a lack of research on the effect of pore size and porous structure on the formation of Ag-NPs. Therefore, we herein report the synthesis of Ag-NPs inside the pores of silica beads (SBs) and assess the effect of their pores on the size and loading amount of Ag-NPs.

2. Materials and methods

2.1. Preparation silica beads

Silica gel was synthesized via a sol–gel method by using sodium silicate ($Na_2O{\cdot}3.4$ SiO2, Shinwoo Materials Co., Ltd.) and 40% H_2SO_4 (Duksan Pure Chemicals Co., Ltd.) as described elsewhere [18]. The obtained gel was aged at various conditions i.e. (1) at acidic low temperature; (2) basic high temperature; and (3) hydrothermal treatment. Accordingly, silica gel aged at pH 9 for 50 h was hydrothermally treated at 180 °C for 5 h to control its pore diameters to about 20 nm [19]. Aging conditions were described in Table 1. The silica gel was dried at 180 °C for 5 h and crushed into beads with sizes ranging from 0.5 to 1 mm. SBs with different pore size ranging from 3.8 t0 19.6 nm were denoted as SBs38, SBs80, SBs130, and SBs200 as given in Table 1.

2.2. Preparation of silver nanoparticle containing silica beads

SBs (2 g) were placed into a 50 ml beaker containing 5 ml of $AgNO_3$ 37 mM (DaeJung Chemical and Metals Co., Ltd.) to generate 1% weight of atomic silver to SiO_2. The beakers were covered and

* Corresponding author. Tel.: +82 31 400 5493; fax: +82 31 500 3579.
E-mail address: khtaik@yahoo.com (H.T. Kim).

0167-577X/$ – see front matter © 2011 Elsevier B.V. All rights reserved.
doi:10.1016/j.matlet.2011.10.073

Table 1
Characteristics of SBs and Ag-NPBs.

Sample	Aging conditions			BET (m^2/g)	Pore volume (cm^3/g)	Pore diameter (nm)	Silver content (%)
	Temperature (°C)	pH	Time (h)				
SBs38	25	1	48	652	0.70	3.8	–
SBs80	80	9	20	417	1.01	7.8	–
SBs130	80	9	50	262	1.14	13.3	–
SBs200	180	9	5	134	0.6	19.6	–
SBA1	–	–	–	597	0.68	3.7	0.13
SBA2	–	–	–	384	0.97	7.6	0.16
SBA3	–	–	–	249	1.04	13.2	0.19
SBA4	–	–	–	134	0.64	19.6	0.11

shook for 3 h at 25 °C. SBs were filtered, quickly washed with 20 ml of deionized water and dispersed into 20 ml of deinonized water in a 100 ml beaker. Then, 10 ml of $NaBH_4$ 50 mM (Duksan Pharmaceutical Co., Ltd.) was added by a dropwise method under mixing conditions. Silver nanoparticles containing silica beads (Ag-NPBs) were removed, washed with deionized water, dried at 100 °C for 4 h. Ag-NPBs were named as SBA1, SBA2, SBA3, and SBA4 corresponding to their silica substrates i.e. SBs38, SBs80, SBs130, and SBs200, respectively. Characterizations were done as described in a previous report [18]. For TEM observation, samples were ground, dispersed in ethanol and then deposited on the copper grid covered with carbon layer and observed with JEOL 2000 FX instrument. The silver loading amount was analyzed using inductively coupled plasma optical emission spectrometry (ICP-730-ES, Varian).

3. Results and discussion

Nitrogen adsorption–desorption method was used to investigate BET surface area and porosity of samples. Fig. 1a presents sorption isotherms, which define the nature of the synthesized materials. The hysteresis loops revealed that SBs80, SBs130, and their silver containing samples have well-defined pore channels, while SBs200 and SBA4 contains less-defined pores. This is in good agreement with pore size distribution shown in Fig. 1b, where SBs80 and SBs130 had relatively narrow pore size distribution; conversely, SBs200 displayed a very wide distribution in pore diameter. The isotherms were quite distinct for SBs38 and SBA1: their desorption brands in hysteresis loops were steeper than the adsorption one. This is associated with a hysteresis loop of type H2, according to IUPAC classification, which indicated that the pore shape of SBs38 is not well-defined or has the possibility of pore blocking effects [20]. TEM images (Fig. S1 in Supplementary materials) indicate that SBs38 has a condense structure with tiny channels, whereas SBs200 contains large pores. Besides, SEM photographs of SBs show that SBs38 are packed with small primary particles. As aging time and temperature increase, the size of the primary particles increases and the opening and larger pores are observed (Fig. S2 in Supplementary materials). After supporting Ag-NPs, BET surface area, pore volume, and pore size of SBs38, SBs80, and SBs130 decreased (Table 1). The decrease is likely due to the deposit of silver particles on their surface and inside pores, which causes the blocks of small channels. Whereas, the SBs200 has large pores, which are not blocked by silver nanoparticles, therefore, their BET surface area and porosity are almost constant.

Representative TEM images of Ag-NPBs suggest that silver nanoparticles were successfully created on free-functionalized SBs (Fig. 2) and size distribution of Ag-NPs in SBA1 and SBA4 does not comply with the pore size distribution in their silica substrates, while the size distribution of Ag-NPs in SBA2 and SBA3 is coincidental with the pore size distribution in their counter SBs, SBs80 and SBs130, respectively (Fig. 1b, inset). To investigate these differences, porous structure and pore size of silica substrate have been taken into account. As seen in Fig. 1b, the average pore size of SBs38 is about 3.8 nm, which is similar to that of

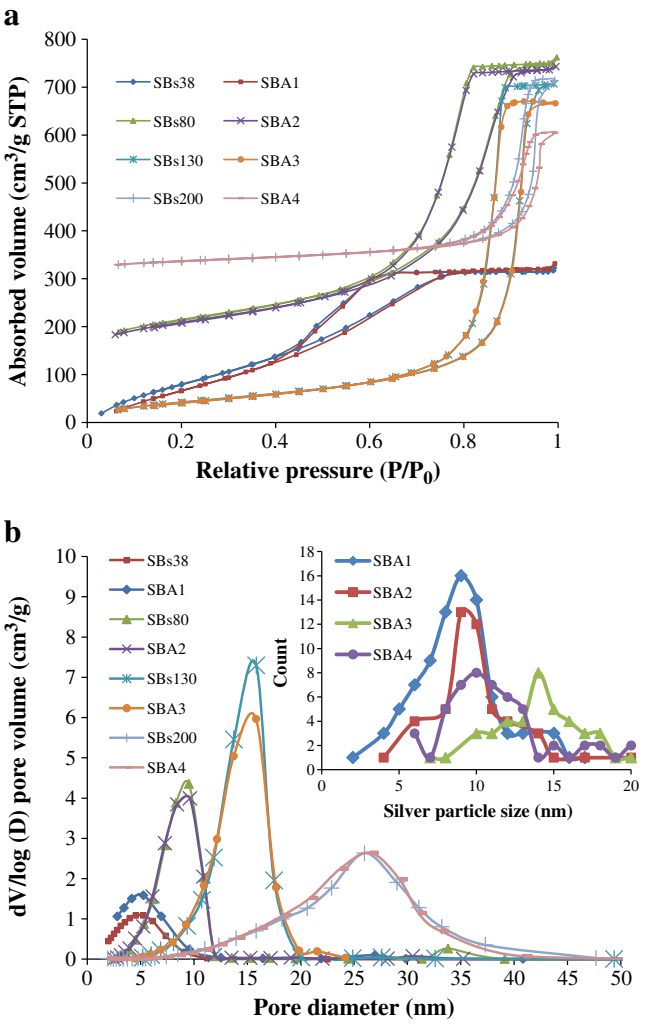

Fig. 1. Nitrogen adsorption–desorption isotherms of the prepared materials (a), pore size distributions measured by the BJH method (a), and size distribution of silver nanoparticles (b, inset).

ordered mesoporous silica, it showed a good capacity to support Ag-NPs [12–14], however, the mean size of Ag-NPs in SBA1 is about 9 nm. Explicitly, Ag-NPs were mostly formed in their large pores. The absence of Ag-NPs in small pores is likely due to their specific porous structure. As discussed, the narrow pore in SBs38 may encounter the pore blocking effects creating ink bottle-like pores [20]. This structure is typically different with that of ordered mesoporous silica, which usually has an open porous structure [21], and therefore, not favorable for Ag^+ ions to percolate into the pores. The sorption hysteresis loop presented in Fig. 1a reflects that SBs200 contains less-defined and large pores, which can be seen in TEM and SEM images (Figs. S1d and S2d in Supplementary materials). The large pores are not good for maintenance of $AgNO_3$ solution. Thus, most silver particles are formed by Ag^+ ions absorbed in small size pores. As mentioned above, SBs80 and SBs130 have well-defined pores, and therefore, are expected to give controllable silver particles. In fact, the distribution of silver particle sizes in SBA2 and SBA3 mostly coincided with pore size distribution of their counter SBs as depicted in Fig. 1b. Unlike pore size, total pore volume does not affect the size of Ag-NPs; however, it has considerable influence on the carrier ability of SBs. As shown in Table 1, silver loading amounts in samples increase along with pore volume. It is evident that the porosity plays an important role in Ag-NPs loading capacity of SBs.

The crystallite of Ag-NPs was investigated by using XRD patterns. In XRD patterns of Ag-NPBs (Fig. 3), diffraction bands at about 23° are attributed to the amorphous structure of SBs. The detected

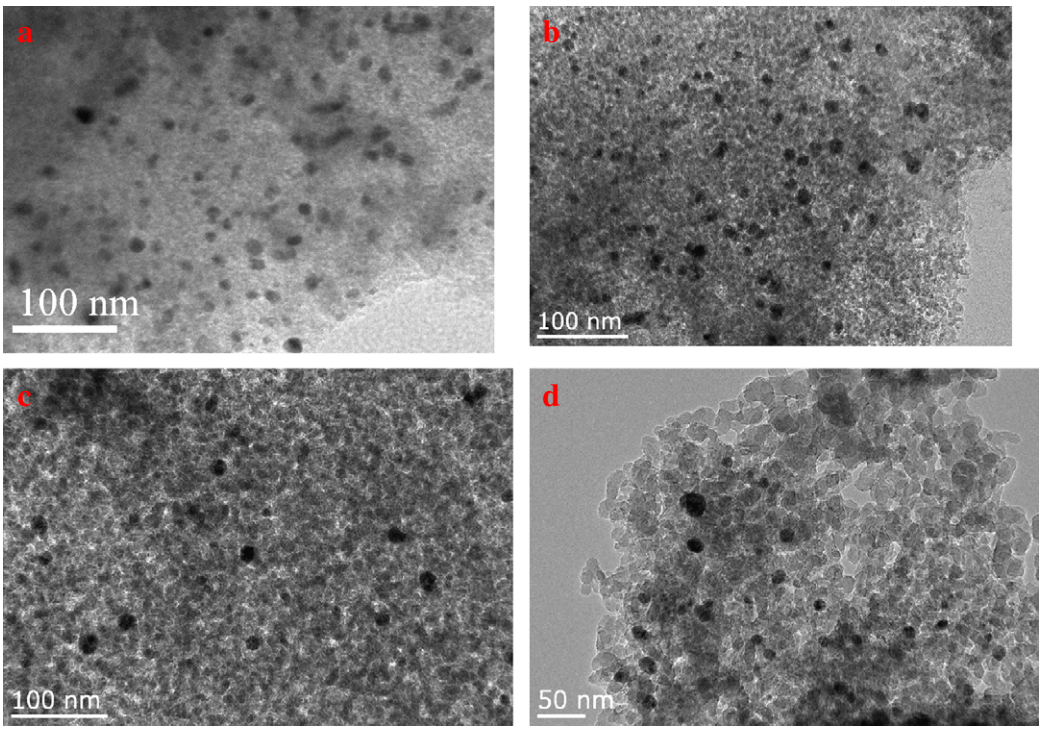

Fig. 2. TEM images of prepared Ag-NPBs: SBA1 (a), SBA2 (b), SBA3 (c), and SBA4 (d).

peaks at 38° belong to reflection of the (111) lattice planes in the face centered cubic structure of silver crystals. The faintness and absence of other diffraction peaks are likely due to the small ratio of Ag-NPs to SBs. However, the peaks obtained indicated the formation of silver crystals in the Ag-NPBs samples.

4. Conclusion

Ag-NPBs were successfully synthesized by manipulating the pore channels inside functionalized-free SBs. The amount and size of resulting Ag-NPs vary with the pore volume and porous structure of SBs, respectively. SBs, which have average pore diameters smaller than 15 nm, well-defined shape pores and are free of a blocking effect, can preserve Ag-NPs within their pores with particle size distribution coinciding with pore size distribution.

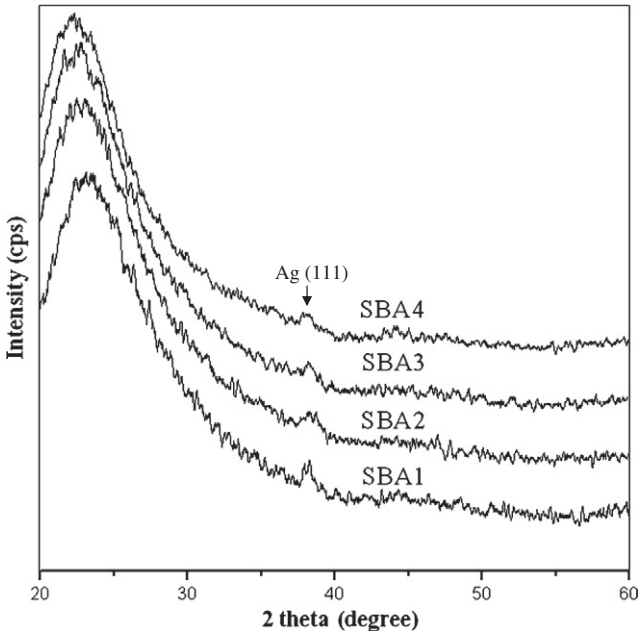

Fig. 3. XRD diffraction patterns of prepared Ag-NPBs.

Acknowledgment

"This study was supported by a grant from the Fundamental R&D Program for Core Technology of Materials funded by the Ministry of Knowledge Economy, Republic of Korea."

Appendix A. Supplementary data

Supplementary data to this article can be found online at doi:10.1016/j.matlet.2011.10.073.

References

[1] Sharma VK, Yngard RA, Lin Y. Silver nanoparticles: green synthesis and their antimicrobial activities. Adv Colloid Interface Sci 2009;145:83–96.
[2] Kiasat AR, Mirzajani R, Ataeian F, Fallah-Mehrjardi M. Immobilized silver nanoparticles on silica gel as an efficient catalyst in nitroarene reduction. Chin Chem Lett 2010;21:1015–9.
[3] Furno F, Morley KS, Wong B, Sharp BL, Arnold PL, Howdle SM, et al. Silver nanoparticles and polymeric medical devices: a new approach to prevention of infection. J Antimicrob Chemother 2004;54:1019–24.
[4] Gangadharan D, Harshvardan K, Gnanasekar G, Dixit D, Popat KM, Anand PS. Polymeric microspheres containing silver nanoparticles as a bactericaidal agent for water disinfection. Water Res 2010;44:5481–7.
[5] Quang DV, Sarawade PB, Hilonga A, Park SD, Kim JK, Kim HT. Facile route for preparation of silver nanoparticle-coated precipitated silica. Appl Surf Sci 2011;257:4250–6.
[6] Chakrabarti K, Whang CM. Silver doped ORMOSIL — an investigation on structural and physical properties. Mater Sci Eng B 2002;88:26–34.
[7] Maroneze CM, LP Da costa, Sigoli FA, Gushikem Y, Mazali IO. One-step preparation of silver nanoparticles confined in functionalized-free SBA-15 channels. Synth Met 2010;160:2099–113.
[8] Ramnani SP, Sabharwal S, Kumar JV, Prasad Reddy KH, Rama Rao KS, Sai Prasad PS. Advantage of radiolysis over impregnation method for the synthesis of SiO_2 supported nano-Ag catalyst for direct decomposition of N_2O. Catal Commun 2008;9:756–61.
[9] Chen W, Zhang J, Di Y, Wang Z, Fang Q, Cai W. Size controlled Ag nanoparticles within pores of monolithic mesoporous silica by ultrasonic irradiation. Appl Surf Sci 2003;211:280–4.

[10] Gurin VS, Petranovskii VP, Hernandez MA, Bogdanchikova NE, Alexeenko AA. Silver and copper clusters and small particles stabilized with nanoparous silicate-based materials. Mater Sci Eng A 2005;391:71–6.
[11] Park JH, Park JK, Shin HY. The preparation of Ag/mesoporous silica by direct silver reduction and Ag/functionalized mesoporous silica by in situ formation of adsorbed silver. Mater Lett 2007;61:156–9.
[12] Pourahmad A, Sohrabnezhad Sh. Preparation and characterization of Ag nanowires in mesoporous MCM-41 nanoparticles template by chemical reduction method. J Alloys Compd 2009;484:314–6.
[13] Adhyapak PV, Karandikar P, Vijayamohanan K, Athawale AA, Chandwadkar AJ. Synthesis of silver nanowires inside mesoporous MCM-41 host. Mater Lett 2004;58: 1168–71.
[14] Zhu W, Han Y, An L. Silver nanoparticles synthesized from mesoporous Ag/SBA-15 composites. Microporous Mesoporous Mater 2005;80:221–6.
[15] Wu PW, Dunn B, Doan V, Schwartz BJ, Yablonovitch E, Yamane M. Controlling the spontaneous precipitation of silver nanoparticles in sol–gel materials. J Sol Gel Sci Technol 2000;19:249–52.
[16] Cai W, Hofmeister H, Reiner T, Chen W. Optical properties of Ag and Au nanoparticles dispersed within the pores of mololithic mesoporous silica. J Nanopart Res 2001;3:443–53.
[17] Bhattacharyya S, Saha SK, Chakravorty D. Silver nanowires grown in the pores of a silica gel. Appl Phys Lett 2000;77:3770–2.
[18] Quang DV, Sarawade PB, Hilonga A, Kim JK, Chai YG, Kim SH, et al. Preparation of silver nanoparticle containing silica micro beads and investigation of their antibacterial activity. Appl Surf Sci 2011;257:6963–70.
[19] Kim JK, Park JK, Kim HK. Synthesis and characterization of nanoporous silica support for enzyme immobilization. Colloids Surf A 2004;241:113–7.
[20] Lowell S, Shields JE, Thomas MA, Thommes M. Characterization of porous solids and powders: surface area, pore size and density. Dordrecht: Kluwer Academic Publishers; 2004.
[21] Huang X, Dong W, Wang Ge, Yang M, Tan L, Feng Y, et al. Synthesis of confined Ag nanowires within mesoporous silica via double solvent technique and their catalytic properties. J Colloid Interface Sci 2011;359:40–6.